

See discussions, stats, and author profiles for this publication at: <https://www.researchgate.net/publication/231371899>

Removal of Hexavalent Chromium From Aqueous Solution Using Low Cost Activated Carbons Derived From Agricultural Waste Materials and Activated Carbon Fabric Cloth

ARTICLE *in* INDUSTRIAL & ENGINEERING CHEMISTRY RESEARCH · JANUARY 2005

Impact Factor: 2.59 · DOI: 10.1021/ie0400898

CITATIONS

220

READS

65

3 AUTHORS, INCLUDING:



Dinesh Mohan

Jawaharlal Nehru University

90 PUBLICATIONS 10,395 CITATIONS

SEE PROFILE

Removal of Hexavalent Chromium from Aqueous Solution Using Low-Cost Activated Carbons Derived from Agricultural Waste Materials and Activated Carbon Fabric Cloth

Dinesh Mohan, Kunwar P. Singh,* and Vinod K. Singh

Environmental Chemistry Division, Industrial Toxicology Research Centre, Post Box No. 80, Mahatma Gandhi Marg, Lucknow 226 001, India

This paper examines an efficient adsorption process for the treatment of tannery wastewater. A variety of low-cost activated carbons were developed from agricultural waste materials, characterized, and utilized for the removal of hexavalent chromium from wastewater. Systematic studies on chromium(VI) adsorption equilibrium and kinetics by low-cost activated carbons as well as commercially available activated carbon fabric cloth were carried out at different temperatures, particle size, pH, and adsorbent doses. Both Langmuir and Freundlich models fitted the adsorption data quite reasonably. The results indicate that the Langmuir adsorption isotherm model fits the data better than the Freundlich adsorption isotherm model. Further, the data are better correlated with the nonlinear form than the linear one. The kinetic studies were conducted to delineate the effects of temperature, initial adsorbate concentration, adsorbent particle size, and solid-to-liquid ratio. The adsorption of Cr(VI) follows pseudo-second-order rate kinetics. On the basis of these studies, various parameters such as the effective diffusion coefficient, activation energy, and activation entropy were evaluated to establish the mechanisms. The adsorption capacities of the tested adsorbents was found to be comparable to those of the available adsorbents/activated carbons.

1. Introduction

Heavy metals can be found in industrial wastewater/effluents from many sources and are deemed undesirable by many researchers/environmentalists. Prolonged exposure to heavy metal ions has been found to cause the degradation of flourishing ecosystems as well as harm to their inhabitants. One heavy metal contaminant that has been a major focus in wastewater management is chromium. Most of the chromium in wastewater, especially hexavalent chromium, is the result of emissions from industries such as electroplating, metal finishing, magnetic tape manufacturing, pigment production, leather tanning, chemical manufacturing, brass making, electrical and electronic equipment manufacturing, and paint and primer pigments manufacturing. For all of these industrial groups, chromium is a problem. Tanning is one of the oldest and fastest growing industries in India. There are about 2161 tanneries in India, excluding cottage industries, that process 500 000 t of hides and skins annually. From these 2161 tanneries, the total annual discharge of wastewater is 9 420 000 m³. The concentration of Cr(VI) found in typical wastewater (such as electroplating or leather tanning wastewater) is in the range of 50–100 mg/L.¹⁶ Chromium, which is on the top-priority list of toxic pollutants defined by the U.S. Environmental Protection Agency (EPA), exists in nature mainly in two oxidation states, 3+ and 6+. It is bioelement in the 3+ state but mutagenic in the 6+ state. Therefore, the speciation of chromium in contaminated environments becomes critical for understanding its fate and exposure. The hydrolysis behavior of Cr(III) is complicated, and it produces mononuclear species CrOH^{2+} , Cr(OH)_2^+ ,

Cr(OH)_4^- , and Cr(OH)_3^0 and the polynuclear species $\text{Cr}_2(\text{OH})_2$ and neutral species $\text{Cr}_3(\text{OH})_4^0$. The hydrolysis of Cr^{6+} produces only neutral and anionic species. The predominate species are CrO_4^{2-} , HCrO_4^{2-} , and $\text{Cr}_2\text{O}_7^{2-}$. At low pH and high chromium concentration, $\text{Cr}_2\text{O}_7^{2-}$ predominates, whereas at pH's greater than 6.5, Cr(VI) exists in the form of CrO_4^{2-} . Chromium(VI) compounds are found to be more toxic than Cr(III) compounds because of the high solubility of Cr(VI) in water and, consequently, its high mobility. Acute exposure to Cr(VI) causes nausea, diarrhea, liver and kidney damage, dermatitis, internal hemorrhaging, and respiratory problems. The drinking water guideline recommended by the U.S. EPA is 100 $\mu\text{g L}^{-1}$. By reviewing the details presented in numerous scientific journals, several metal ion reduction techniques have become targeted as possible solutions. Ion exchange,^{1,2} reduction,³ chemical precipitation,⁴ polymer-based filtration, membrane separation,^{5,6} adsorption,^{7,8} electrochemical precipitation,⁹ solvent extraction,¹⁰ cementation,¹¹ and electrokinetic remediation¹² are among the available methods for effectively accomplishing metal concentration reduction. Nevertheless, many of these approaches are marginally cost-effective or difficult to implement in developing countries. Therefore, the need exists for a treatment strategy that is simple and robust and that addresses local resources and constraints. Adsorption can be an effective and versatile method for removing chromium, particularly when combined with appropriate regeneration steps. This solves the problems of sludge disposal and renders the system more economically viable, especially if low-cost adsorbents are used.

A variety of activated carbons are available commercially, but very few of them are selective for heavy metals and most are very costly. Despite the prolific use of carbon adsorbent^{8,13,14} for wastewater treatment, carbon adsorption is an expensive treatment process, and

* To whom correspondence should be addressed. E-mail: dm_1967@hotmail.com. Tel.: 0091-522-2508916. Fax: 0091-522-2628227.

there is a definite need for improved and tailor-made materials to suit these demanding applications. A substitute for activated carbons should be readily available and economically feasible, and above all, it should be able to be regenerated chemically with simultaneous quantitative recovery of the adsorbate material. The past 10 years has seen a developing interest in the preparation of low-cost adsorbents as alternatives to activated carbon in water and wastewater treatment processes.

In several previous reports, many investigators have studied the feasibility of less expensive materials such as alginate beads,¹⁵ wheat straw,¹⁶ carbon developed from waste materials,^{17–20} biosorbents,^{21–23} activated sludge,²⁴ bagasse fly ash,²⁵ blast furnace waste,²⁶ coals,²⁷ bone charcoal,⁷ biogas residual slurry,²⁸ copper smelting slag,²⁹ red mud,³⁰ and agricultural waste.³¹ for the removal of chromium from water/wastewater. However, the problems associated with these adsorbents are the regeneration and recovery of the useful materials, which made them unattractive for wider commercial applications. This calls for a research effort to develop an industrially viable, cost-effective, and environmentally compatible technology for the removal of chromium from wastewater. For quite some time we have been involved in developing some low-cost activated carbons/adsorbents for the removal and recovery of organics/metal ions from wastewater.^{32–37} Continuing our activities in this direction, we have derived a variety of low-cost activated carbons from agricultural waste materials such as coconut shell fibers and coconut shell and used them for the removal of hexavalent chromium from synthetic wastewater. A commercially available activated carbon cloth fabric (ACF) was also studied for the removal of chromium from water/wastewater.

2. Materials and Methods

All reagents were AR-grade chemicals. The pH of the test solutions was adjusted using AR-grade dilute H₂SO₄ (0.1 N) and NaOH (0.1 N). The stock solution of hexavalent chromium was prepared by dissolving K₂Cr₂O₇ in doubly distilled water.

2.1. Equipment. The pH measurements were made using a pH meter (model 744, Metrohm). The conductivity of the water was measured on a model Thermo Orion 162A conductivity meter. X-ray measurements were made using a Phillips X-ray diffractometer employing nickel-filtered Cu K α radiation. Scanning electron microscopy was performed using a Philips XL-20 electron microscope. The carbons were characterized in terms of chemical composition by carrying out proximate and elemental analyses and also texturally by performing gas adsorption, mercury porosimetry, and helium and mercury density measurements. Information on chemical structure was obtained by recording the infrared spectrum of the carbons in potassium bromide and Nujol mull in the range of 500–4000 cm⁻¹ using a Perkin-Elmer spectrophotometer. The values of the BET specific surface area (S_{BET}) and pore volumes (micropore volumes, V_{mi} and W_0 ; mesopore volumes, V_{me} and $V_{\text{me-p}}$; macropore volume, $V_{\text{ma-p}}$; and total pore volume, V_{T}) were determined using a Quantachrome model Autosorb-1 surface area analyzer. The mercury porosimetry have been carried out with a Quantachrome model Autoscan-60 porosimeter. The mercury density was determined as usual, by carrying out the mercury porosimetry experiments. The helium density was measured using a Quantachrome stereopycnometer. The

chemical constituents of the activated carbon were analyzed following the standard methods of chemical analysis.^{32,38} The metal concentrations in the liquid samples were determined using an atomic absorption spectrophotometer (AAS, model Perkin-Elmer 3100). Agitation of the system under investigation was carried out on a thermostat-cum-shaking assembly (model NSW-133).

2.2. Quality Assurance/Quality Control. To establish the accuracy, reliability, and reproducibility of the collected data, all batch isotherm tests were replicated twice, and experimental blanks were run in parallel. The AAS was operated at the wavelength providing the optimum sensitivity for chromium. Multiple sources of National Institute of Standard and Technology (NIST) traceable standards were used for instrument calibration and standard verification. Dilutions were made with 2% HNO₃, and > 18-M Ω resistivity water was used in all tests. All jars, conical flasks, and containers used in the study were prepared by being soaked in 5% HNO₃ for a period of 3 days before being triply rinsed with distilled, deionized water and oven dried. The precision of the analytical procedures expressed as the relative standard deviation (RSD) ranged from 5 to 10%. The precision for the analysis of standard solution was better than 5%. Recoveries of metals from the samples were also studied for evaluation of matrix effects by the standard addition technique and found to be between 94 and 106%. In different experiments, blanks were run, and corrections were applied if necessary. All observations were recorded in triplicate, and average values and their standard deviations are reported.

Linear and nonlinear regression analyses were applied to each set of data points. A correlation coefficient (R^2) and a probability value (p) representing the “goodness of fit” of the Freundlich and Langmuir models to the data were obtained by both the linear and nonlinear regression programs using Sigma Plot V6.0 for Windows (SPSS Inc., Chicago, IL).

2.3. Adsorbent Development. Coconut shell (agricultural waste), a hard and thick bony endocarp material that, together with the coconut shell fibers, often presents serious disposal problems for local environments, is available abundantly. These raw materials, i.e., coconut shell fibers and coconut shells, were collected locally from Lucknow, India. Two different classes of carbonaceous materials were prepared. Class I carbons were prepared by treating 1 part coconut shell fibers and coconut shell with 2 parts (by weight) concentrated sulfuric acid separately and keeping them in an oven maintained at 150–165 °C for a period of 24 h. The carbonized materials were washed well with doubly distilled water to remove the free acid and dried at 105–110 °C for 24 h. Dried coconut shell fibers and coconut shells were subjected to thermal activation at different temperatures, viz., 200, 400, 600, and 800 °C, for 1 h in an inert atmosphere. Class II carbons were prepared by simply activating the coconut shell fibers and coconut shells without any chemical treatment at different temperatures (200, 400, 600, and 800 °C) in an inert atmosphere. The temperature and time were optimized by observing the surface properties of the activated products obtained. In both cases (with and without chemical treatment), the products obtained at temperatures higher or lower than 600 °C exhibited poor adsorption capacities. The temperature and time were

optimized by observing the surface properties of the activated products obtained by treating the raw materials for different intervals of time at varying temperatures mentioned above. The products so obtained were sieved to the desired particle sizes such as 30–200, 200–250, and 250–300 mesh. The carbon having the 30–200 mesh size was used in both the sorption and kinetic studies unless otherwise stated. Finally, the product was stored in a vacuum desiccator until required. The developed carbons are designated as FAC (activated carbon derived from coconut fibers), SAC (activated carbon derived from coconut shells), ATFAC (activated carbon derived from acid-treated coconut fibers), and ATSAC (activated carbon derived from acid-treated coconut shells). In addition to these samples, a commercially available activated carbon fabric cloth (ACF) was used for the removal of Cr(VI). The ACF was obtained from HEG Limited, Mandideep, Bhopal, India. According to the manufacturer, the activated carbon fabric was prepared by carbonization of a precursor in an inert atmosphere after suitable chemical treatment. This activation was carried out under closely controlled conditions to obtain optimum properties.

2.4. Sorption Procedure. Sorption studies were performed by the batch technique to obtain rate and equilibrium data. The batch technique was selected because of its simplicity. Batch sorption studies were performed at different temperatures, particle sizes, and adsorbent doses to obtain equilibrium isotherms and data required in the design and operation of column reactors for the treatment of Cr(VI)-bearing wastewater. For isotherm studies, a series of 100-mL conical flasks were employed. Each conical flask was filled with 50 mL of Cr(VI) solution of varying concentrations (1–100 mg/L) and adjusted to the desired pH and temperature. The concentration range of 1–100 mg/L was chosen on the basis of a good deal of preliminary investigations and in accordance with the levels of chromium generally present in wastewater/industrial effluents. A known amount of adsorbent (0.1 g) was added to each conical flask, and the mixture was agitated intermittently for the desired time periods, up to a maximum of about 48 h. The contact time and other conditions were selected on the basis of preliminary experiments, which demonstrated that equilibrium was established in 48 h. Equilibration for longer times between 48 and 72 h gave practically the same uptakes. Therefore, a contact period of 48 h was finally selected for all equilibrium tests. After this period, the solution was filtered using Whatman no. 42 filter paper and analyzed by atomic absorption spectrometry for the concentration of Cr(VI) remaining in the solution. The effect of pH was observed by studying the adsorption of Cr(VI) over a broad pH range of 2–10. The sorption studies were also carried out at different temperatures, i.e., 10, 25, and 40 °C, to determine the effect of temperature and to evaluate the sorption thermodynamic parameters. Adsorption of Cr(VI) was also studied at different doses of adsorbent and different particle sizes. The concentration of Cr(VI) retained in the adsorbent phase was calculated as the difference between the original concentration of the solution and the measured concentration in solution after equilibrium. The mass balance can be expressed as

$$W(q_e - q_0) = V(C_0 - C_e) \quad (1)$$

When $q_0 = 0$, eq 1 becomes equivalent to

Table 1. Compositions and pH's of Activated Carbons Derived from Agricultural Waste Materials

sample	ash (%)	C (%)	N (%)	H (%)	pH
SAC	68.23	69.23	0.25	2.21	7.02
ATSAC	62.65	76.64	0.28	2.26	5.72
FAC	71.23	71.54	0.32	1.83	7.80
ATFAC	72.28	76.38	0.38	1.95	5.80

$$q_e = \frac{(C_0 - C_e)V}{W} \quad (2)$$

where q_0 and q_e are the initial and equilibrium concentrations, respectively, of Cr(VI) on the adsorbent (mg/g); C_0 and C_e are correspondingly the initial and equilibrium concentrations of Cr(VI) in solution (mg/L); V is the volume (L); and W is the weight (g) of the adsorbent.

2.5. Kinetic Studies. Successful application of the adsorption technique demands the development of cheap, nontoxic, readily available adsorbents with known kinetic parameters and sorption characteristics. Foreknowledge of the optimal conditions would enable better design and modeling of the process. Thus, the effects of some major parameters, viz., contact time, amount and particle size of adsorbent, and concentration of adsorbate, were studied using the bench technique. A number of stoppered flasks (100-mL capacity) containing 50 mL of a 50 mg/L solution of Cr(VI) were placed in a thermostat-cum-shaking assembly. When the desired temperature was reached, 0.1 g of activated carbon was added into each flask, and the solutions were agitated by mechanical shaking. At predetermined intervals of time, the solutions of specified conical flasks were separated from the activated carbon and analyzed for the uptake of Cr(VI). The amount of Cr(VI) adsorbed was calculated using eq 2.

3. Results and Discussion

3.1. Characterization. For characterization of the prepared activated carbons, 1.0 g of each was stirred with deionized water (100 mL, pH 6.8) for 2 h and left for 24 h in an airtight stoppered conical flask. After the equilibration time of 24 h, the change in the pH was recorded (Table 1). The carbon is quite stable in water, salt solutions, dilute acids, dilute bases, and organic solvents. The specific surface area of the carbons was evaluated from the N_2 isotherms by applying the Brunauer, Emmett, and Teller (BET) equation at a relative pressure (P/P_0) of 0.35 and an average area per molecule of N_2 in a completed monolayer (a_m) of 16.2 Å. The micropore volume was obtained from the aforementioned isotherms as well by taking it as being equal to the volume of N_2 adsorbed at $P/P_0 = 0.10$ (V_{mi}) and was also determined by applying the Dubinin–Radushkevich equation (W_0). V_{mi} and W_0 are expressed as liquid volumes. The volumes of mesopores (V_{me}) and macropores (V_{ma}) were derived from plots of the cumulative pore volume (V_{cu}) against the pore radius (r) (mercury porosimetry): $V_{me} = V_{cu}$ (at $r = 10$) – V_{ma} and $V_{ma} = V_{cu}$ (at $r = 250$ Å). The total pore volume was calculated by making use of the expression $V_T = 1/\rho_{Hg} - 1/\rho_{He}$, where ρ_{Hg} and ρ_{He} are the mercury and helium densities, respectively, and also by summing the volumes V_{mi} , V_{me} , and V_{ma} . The values of S_{BET} , V_{mi} , W_0 , V_{me} , ρ_{Hg} , ρ_{He} , V_T , and V_T' are listed in Table 1. The IR and SEM studies were restricted to only samples ATFAC and ATSAC. The carbonaceous materials, viz., FAC and SAC, were chosen just for comparison of the sorption results. The

Table 2. Characteristics^a [S_{BET} , Microporosities (N_2 at 77 K), Pore Volumes, and Densities] of Activated Carbons Derived from Agricultural Waste Materials

sample	S_{BET} (m^2/g)	V_{mi} ($\text{cm}^3 \text{g}^{-1}$)	W_0 ($\text{cm}^3 \text{g}^{-1}$)	V_{me} ($\text{cm}^3 \text{g}^{-1}$)	V_{ma} ($\text{cm}^3 \text{g}^{-1}$)	ρ_{Hg} (g cm^{-3})	ρ_{He} (g cm^{-3})	V_{T} ($\text{cm}^3 \text{g}^{-1}$)	V'_{T} ($\text{cm}^3 \text{g}^{-1}$)
SAC	378	0.12	0.12	0.05	0.09	1.54	0.98	0.37	0.36
ATSAC	380	0.12	0.13	0.05	0.19	1.60	0.91	0.47	0.26
FAC	343	0.10	0.11	0.03	0.89	1.58	0.49	1.41	1.02
ATFAC	512	0.17	0.18	0.07	0.29	1.65	0.84	0.58	0.53

^a $V_{\text{me}} = V_{\text{cu}}(\text{at } r = 20 \text{ \AA}) - V_{\text{ma}}$, $V_{\text{ma}} = V_{\text{cu}}(\text{at } r = 250 \text{ \AA})$, V_{cu} = cumulative pore volume (mercury porosimetry), $V_{\text{T}} = 1/\rho_{\text{Hg}} - 1/\rho_{\text{He}}$, $V'_{\text{T}} = V_{\text{mi}} + V_{\text{me}} + V_{\text{ma}}$.

Table 3. Properties of Activated Carbon Fabric Cloth

property	value
surface area (S_{BET} , m^2/g)	1565
pore volume (cm^3/g)	0.65
effective pore size (\AA)	< 8.0
thickness (mm)	7–9
density (g/cm^3)	0.2–0.7
decomposition temp ($^{\circ}\text{C}$)	> 500
width (cm)	60/87
texture	plain
pH	7.0
hydrogen (%)	0.80
carbon (%)	80

chemical components and characteristics of the activated carbons are reported in Tables 1 and 2, respectively, and the complete characterization of ACF³⁹ is provided in Table 3.

The X-ray diffraction analysis (figure omitted for brevity) of the activated carbons did not show any peaks, thereby indicating the amorphous nature of the carbons prepared from coconut shell and coconut shell fibers.

The carbon percentage yield was calculated using the following equation

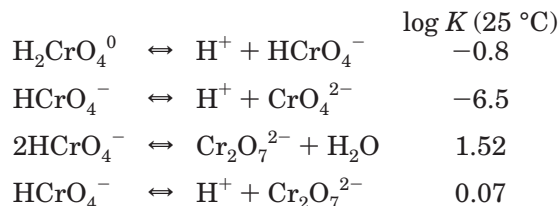
$$\text{carbon yield (\%)} = \frac{\text{weight after carbonization (g)}}{\text{weight before carbonization (g)}} \times 100$$

The identification of various constituents in the different forms of activated carbon, viz., ATFAC and ATSAC, was done with the help of IR spectra (Figure 1a,b). The IR spectra of the activated carbons showed weak and broad peaks in the region of 3853–453 cm^{-1} . Approximate FT-IR band assignments indicated the presence of carbonyls, carboxyls, lactones, and phenols. The 1800–1540 cm^{-1} band is associated with C=O stretching mode in carbonyls, carboxylic acids, and lactones, whereas the 1440–1000 cm^{-1} band was assigned to the C–O stretching and O–H bending modes in phenols and carboxylic acids. The assignment of a specific wavenumber to a given functional group was not possible because the absorption bands of various functional groups overlap and shift, depending on their molecular structure and environment. The overlapping and shifting is greater in the ATFAC carbon than in the ATSAC carbon. Shifts in absorption positions can be caused by factors such as intramolecular and intermolecular hydrogen bonding, steric effects, and degrees of conjugation. For instance, within its given range, the position of the C=O stretching band (common to carbonyls, carboxylic acids, and lactones) is determined by many factors. These include (i) the physical state, (ii) electronic and mass effects of neighboring substituents, (iii) conjugation, (iv) hydrogen bonding, and (v) ring strain. The IR absorption bands of oxygen groups on the surface of solid GAC are likely to be affected by some or all of these same factors. Although some inference can be made

about the surface functional groups from the IR spectra, the weak and broad bands do not provide any authoritative information about the nature of surface oxides.

Scanning electron microscopy (SEM) images of ATFAC and ATSAC³² at different magnifications revealed the surface textures and different levels of porosity in the prepared activated carbons under study. It was concluded that there were considerable small cavities, cracks, and attached fine particles over the activated carbon surface, forming a system of complicated pore networks. It was also noticed that the carbon particles were in the form of spherical particles of a wide range of sizes.

3.2. Sorption Studies. pH is the one of the most important parameters controlling the metal ion sorption process. The effect of pH on the adsorption of chromium is attributed to interactions between ions in solution and complexes formed at the adsorbent surface. The fact that Cr(VI) in aqueous solution can form different species in the solution at various pH's is very well documented in literature. The speciation diagram for chromium(VI) can be obtained using the following reactions and equilibrium constants⁴⁰



The removal of Cr(VI) as a function of pH together with the equilibrium pH is presented in Figure 2. These studies were carried out at the initial concentration of 50 mg/L. The adsorption of Cr(VI) on the prepared adsorbents decreases with increasing pH_{in} . Figure 2 shows that the prepared carbons as well as the activated carbon fabric cloth are active in the acidic range and especially in the low pH range. The maximum adsorption of Cr(VI) species on the various adsorbents was found to be at pH 2.0 and negligible at pH values over 8. Cr(VI) can exist in several stable forms such as CrO_4^{2-} , HCrO_4^- , $\text{Cr}_2\text{O}_7^{2-}$, and HCr_2O_7^- , and the relative abundance of a particular complex depends on the concentration of the chromium ion and the pH of the solution. At low pH, the sorbent is positively charged because of the protonation, whereas the sorbate, dichromate ions, exists mostly as an anion, leading to an electrostatic attraction between the sorbent and sorbate. This results in increased adsorption at low pH. As the pH of the solution increases, the sorbent undergoes deprotonation, and the adsorption capacity decreases. Therefore, all subsequent studies were carried out at pH 2.0.

The following equation shows the equilibrium relationship between the different chromium anions

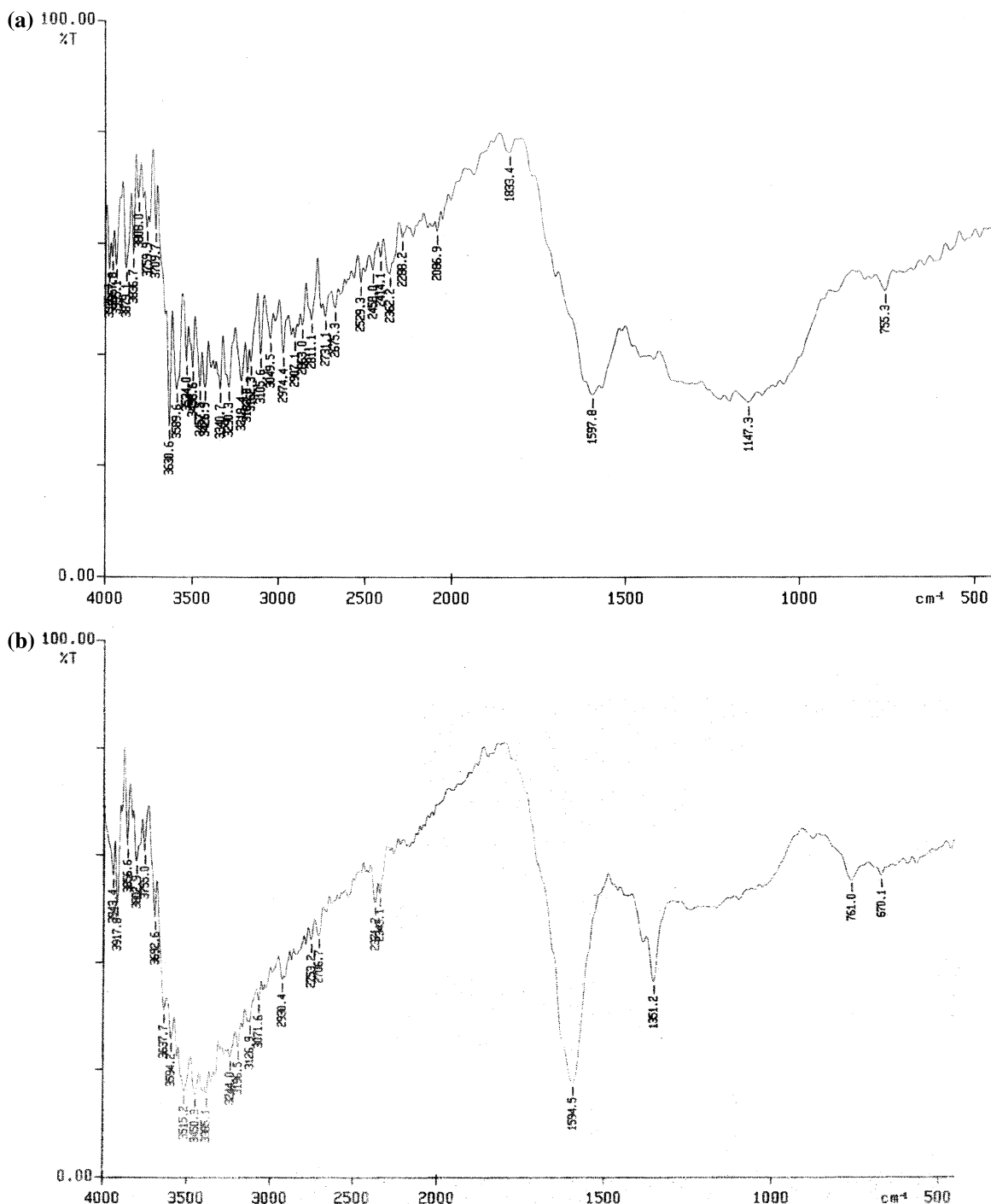


Figure 1. IR spectrum of activated carbons derived from coconut shell fibers and coconut shell: (a) ATFAC and (b) ATSAC.



It is interesting to note that the equilibrium pH does not change much in the acidic pH range, whereas it decreases in the basic pH range, as can be seen from Figure 2. The high removal of Cr(VI) at low pH was also reported earlier by us^{25,26} on different adsorbents and by others.^{18,19,21,41} The adsorption of hexavalent chromium on a carbonaceous material developed from the waste slurry of a fertilizer plant, as studied by Srivastava et al.,²⁶ was found to be greater at pH values of 2.0 or less. Almost 100% removal was reported at lower concentrations, which is very similar to the current findings. An excellent explanation of Cr(VI) adsorption on various adsorbents was provided by Rodovic et al.⁴²

The isotherms (data points) for adsorption of the Cr(VI) at the optimum pH (2.0) of adsorption on activated carbons developed from agricultural waste materials are shown in Figures 3–7 at three different temperatures. The isotherms are positive, regular, and concave to the concentration axis. In all cases, the uptake of Cr(VI) increases with increasing temperature, thereby indicating that the process is endothermic in nature. The increase in adsorption of chromium(VI) in the form of chromate ions with temperature is probably a combination of “activated diffusion” plus an increase in surface area caused by oxidation associated with the observed reduction of chromate ions on the surface of carbonaceous material. Such activated adsorption would widen and deepen the very small micropores, i.e., cause

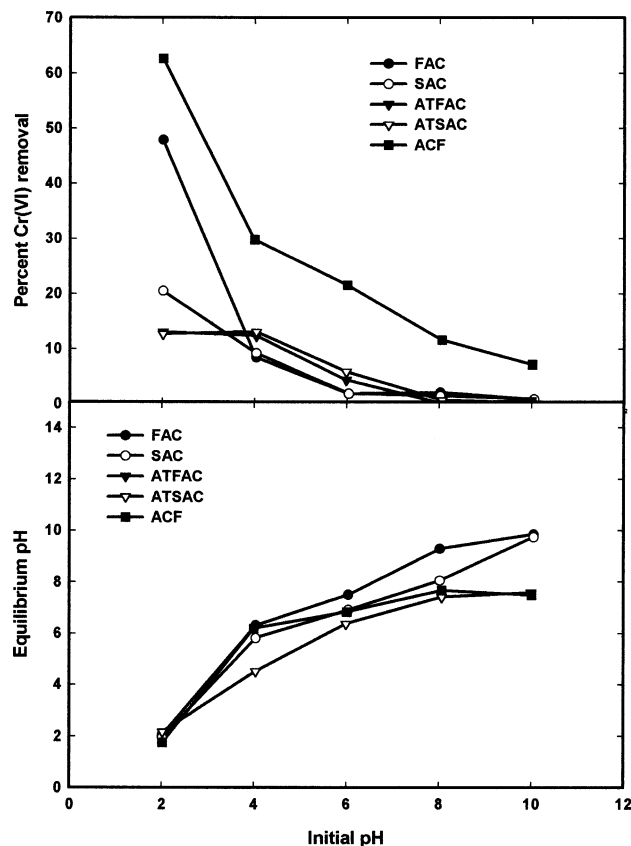


Figure 2. Effect of pH on the adsorption of Cr(VI) by various adsorbents at 25 °C and an adsorbate concentration of 50 mg/L.

“pore burrowing”, and so create more surface for adsorption. The uptake of Cr(VI) by various adsorbents is almost 100% at low adsorbate concentrations, whereas it same decreases when the adsorbate concentrations are higher, as can be seen from Figures 3–7. The adsorption studies were carried out at 10, 25, and 40 °C to determine the adsorption isotherms, and the isotherm parameters were evaluated using linear and nonlinear Langmuir and Freundlich models as given by eqs 3–6. The use of linearized equations apparently produces large errors in the parameters. This problem is related to complications arising from the simultaneous transformation of measurement errors with data. The Langmuir adsorption isotherm predicts the formation of an adsorbed solute monolayer, with no site interactions between the adsorbed ions. It also assumes that the interaction takes place by adsorption of one ion per binding site and that the sorbent surface is homogeneous and contains only one type of binding site. On the other hand, the Freundlich model does not predict surface saturation. It considers the existence of a multilayered structure.

Langmuir Isotherm. The Langmuir equation can be written as

$$q_e = \frac{Q^0 b C_e}{1 + b C_e} \quad (\text{nonlinear form}) \quad (3)$$

$$\frac{C_e}{q_e} = \left(\frac{1}{Q^0 b} \right) + \left(\frac{1}{Q^0} \right) C_e \quad (\text{linear form}) \quad (4)$$

where q_e is the amount of solute adsorbed per unit weight of adsorbent (mg/g), C_e is the equilibrium concentration of solute in the bulk solution (mg/L), Q^0

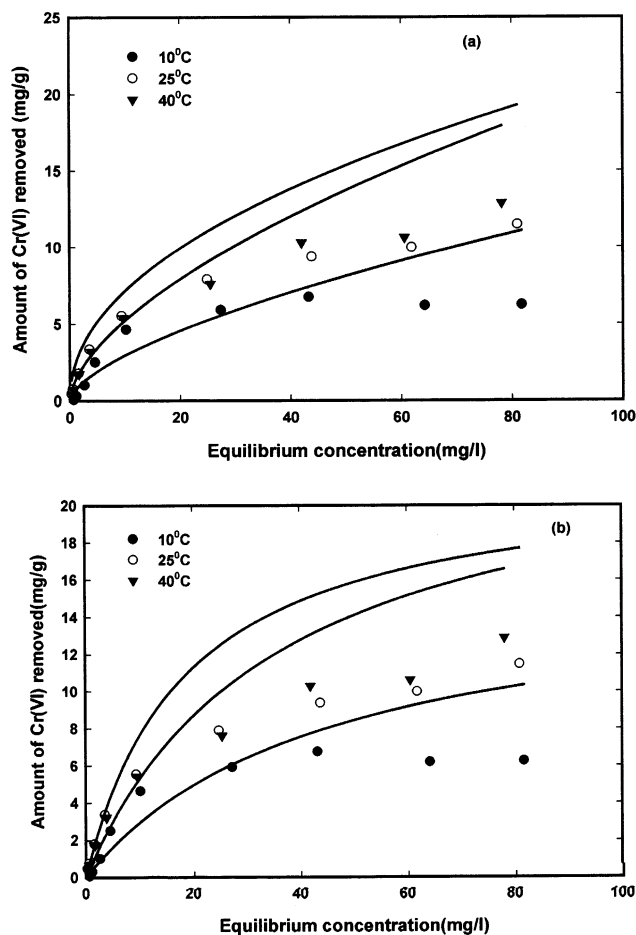


Figure 3. Adsorption of Cr(VI) on activated carbon derived from coconut shell fiber without acid treatment (FAC) at different temperatures and at pH 2.0. Solid lines represent the fitting of the data by the (a) Freundlich and (b) Langmuir isotherms.

is the monolayer adsorption capacity (mg/g), and b is a constant related to the free energy of adsorption ($b \propto e^{-\Delta G/RT}$). Its value is the reciprocal of the concentration at which half-saturation of the adsorbent is reached.

Freundlich Isotherm. The Freundlich equation can be written as

$$q_e = K_F C_e^{1/n} \quad (\text{nonlinear form}) \quad (5)$$

$$\log q_e = \log K_F + \frac{1}{n} \log C_e \quad (\text{linear form}) \quad (6)$$

where q_e is the amount of solute adsorbed per unit weight of adsorbent (mg/g), C_e is the equilibrium concentration of solute in the bulk solution (mg/L), K_F is a constant indicative of the relative adsorption capacity of the adsorbent (mg/g), and $1/n$ is a constant indicative of the intensity of the adsorption.

The nonlinear Freundlich and Langmuir isotherms for the adsorption of Cr(VI) on the prepared activated carbons together with ACF at different temperatures are also presented in Figures 3–7. The solid lines represent the lines of model fits over a wide range of concentrations. The corresponding Freundlich and Langmuir parameters along with correlation coefficients are reported in Tables 4 and 5, respectively. The correlation coefficients indicate (Tables 4 and 5) that, in general, the Langmuir model fit the results better than the Freundlich model, although the values of R^2 are not very

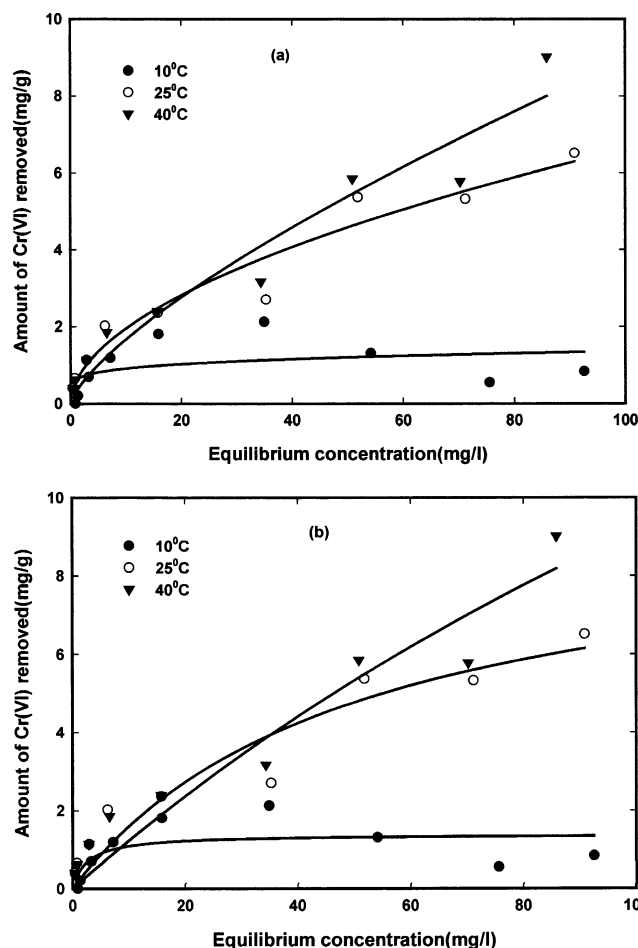


Figure 4. Adsorption of Cr(VI) on activated carbon derived from coconut shell without acid treatment (SAC) at different temperatures and at pH 2.0. Solid lines represent the fitting of the data by the (a) Freundlich and (b) Langmuir isotherms.

high, which is further verified by a plot between the regression coefficients of Freundlich and Langmuir models. It is clear from Figure 8 that the Langmuir model has better regression coefficients. This might be due to the change in the mechanism of adsorption with concentration. In the case of ACF, the data cannot be modeled by the Langmuir isotherm where a negative value of b is obtained.

The monolayer adsorption capacity (Q^0) for Cr(VI), as calculated from the nonlinear Langmuir isotherms, was found to be relatively higher for the activated carbons prepared without any chemical treatment in comparison to those obtained by acid treatment.

Further, the sorption capacities of the carbons developed from coconut shell fibers are higher than that of the carbons prepared from coconut shell. Among the adsorbents studied for the removal of Cr(VI), the activated carbon cloth has the largest surface areas, resulting in the highest uptake of the chromium. Activated carbon fibers have only micropores that are directly accessible from the external surface of the fiber, and therefore, the chromate ions reach adsorption sites through micropores without the additional diffusion resistance of macropores, which is usually the rate-controlling step in the case of granular adsorbents. Also, the activated carbon fibers (ACFs) have a high carbon content and preferentially adsorb Cr(VI). Surface area is not the only criterion, and other factors such as precipitation, surface complexation, and ion exchange

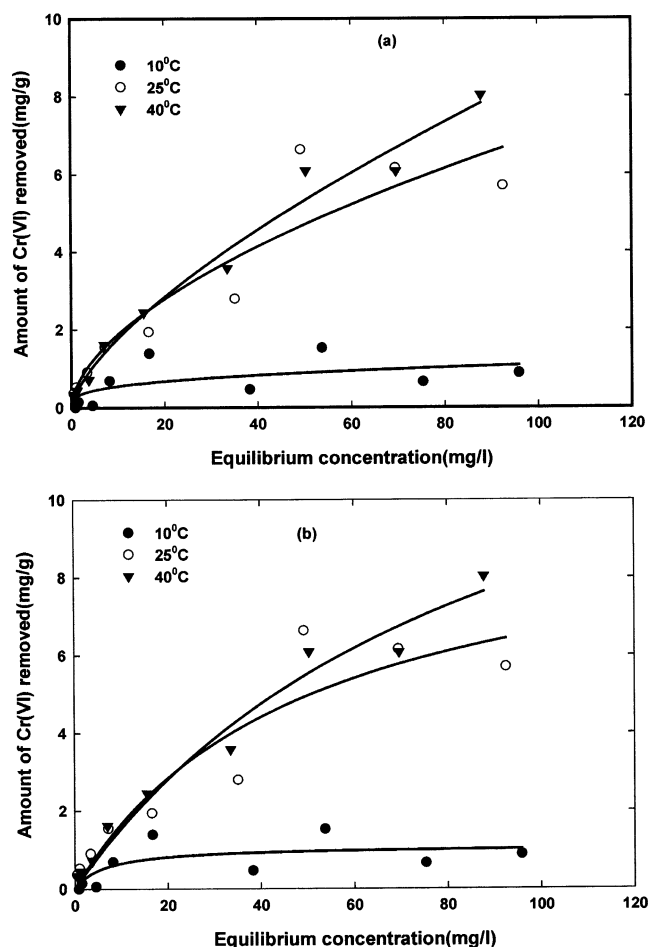


Figure 5. Adsorption of Cr(VI) on activated carbon derived from coconut shell fibers with acid treatment (ATFAC) at different temperatures and at pH 2.0. Solid lines represent the fitting of the data by the (a) Freundlich and (b) Langmuir isotherms.

also play an important role in the adsorption of Cr(VI) on the developed adsorbents.

The essential characteristic of a Langmuir isotherm can be expressed in terms of a dimensionless constant separation factor, R_L , which was defined by Weber and Chakravorti⁴³ and applied earlier by us^{33,34} on different systems, as given by

$$R_L = \frac{1}{1 + bC_0} \quad (7)$$

where b (L/mg) is the Langmuir constant; C_0 (mg/L) is the initial concentration; and R_L indicates the shape of the isotherm as given in Figure 9, with Q_e the amount of chromium adsorbed (mg/g) on the prepared adsorbents and C_e the equilibrium concentration of chromium in solution.

Types of equilibrium isotherm are related to the R_L values as follows:

$$\begin{array}{ll} R_L > 1 & \text{unfavorable} \\ R_L = 1 & \text{linear} \\ 0 < R_L < 1 & \text{favorable} \\ R_L > 0 & \text{irreversible} \end{array}$$

The dimensionless separation factor, R_L , was determined at different temperatures, particle sizes, and adsorbent doses over a broad concentration range. The values

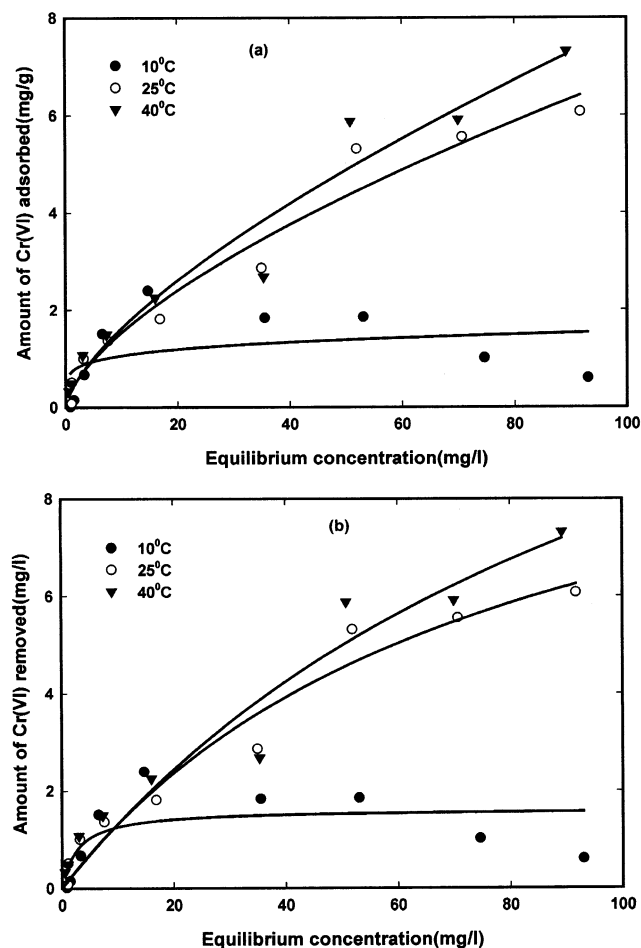


Figure 6. Adsorption of Cr(VI) on activated carbon derived from coconut shell with acid treatment (ATSAC) at different temperatures and at pH 2.0. Solid lines represent the fitting of the data by the (a) Freundlich and (b) Langmuir isotherms.

of R_L at different particle sizes, adsorbent doses, and temperatures were found to be greater than 0 and less than 1, indicating the favorable adsorption of Cr(VI) on activated carbons derived from various agricultural waste materials (data omitted for brevity). The degree of favorability is generally related to the irreversibility of the system, giving a qualitative assessment of the carbon–chromium and cloth–carbon interactions. The degrees tended toward zero (the completely ideal irreversible case) rather than unity, which represents a completely reversible case. In the case of ACF, the values of $R_L > 1$ further confirm the unfavorability of the isotherms.

3.3. Kinetic Studies. The kinetics or rates of reactions are an important aspect of environmental chemistry, especially with regard to understanding the speciation of chemicals. An understanding of the reaction rates of environmental processes allows for the calculation of speciation using an equilibrium model, a

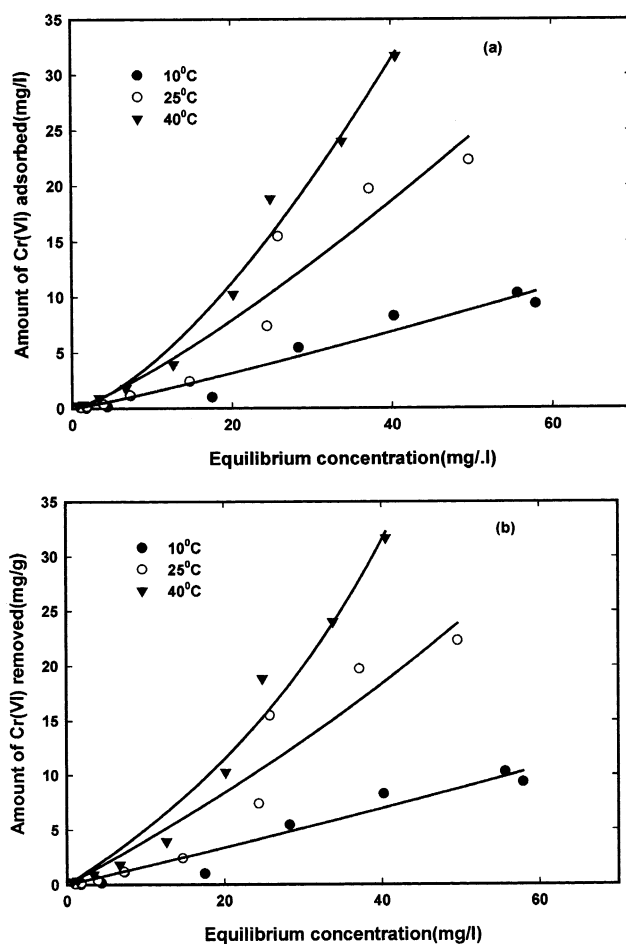


Figure 7. Adsorption of Cr(VI) on activated carbon fabric cloth (ACF) at different temperatures and at pH 2.0. Solid lines represent the fitting of the data by the (a) Freundlich and (b) Langmuir isotherms.

nonreaction model, or an intermediate model in which kinetics must be considered. Studies of the kinetics of Cr(VI) were carried out only on FAC and ACF as these adsorbents show excellent sorption capacities in terms of Q^0 as compared to SAC, ATFAC, and ATSAC at different temperatures (Table 5).

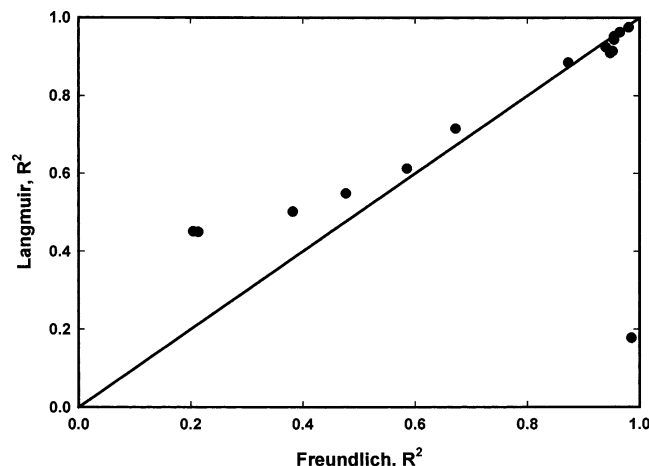
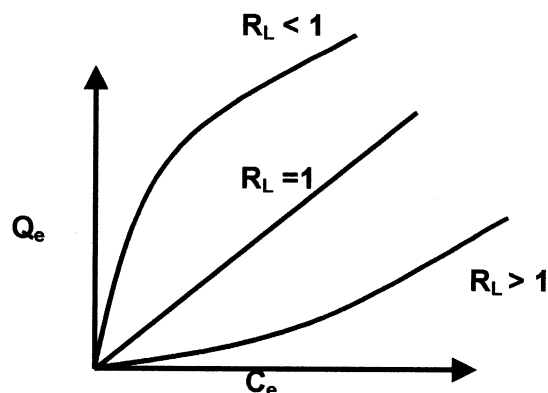
The effect of the amount of adsorbent on the rate of uptake of Cr(VI) was studied at 0.05, 0.1, and 0.2 g. The uptake increased with increasing amount of the adsorbent material (figure omitted for brevity). There is a substantial increase in the adsorption when the carbon dosage increases from 0.05 to 0.1 g, whereas the increase upon introducing an additional 0.1 g of carbon is not as significant. Keeping this result in view, the amount of carbon was kept at 0.1 g per 50 mL or 2 g/L in all subsequent kinetic studies. Further the half-life of the process (t_{50}) decreases with increasing amount of adsorbent, confirming that the rate of adsorption is

Table 4. Freundlich Isotherm Constants for Cr(VI) Adsorption on Activated Carbons Derived from Agricultural Waste Materials and Activated Carbon Fabric Cloth at Different Temperatures

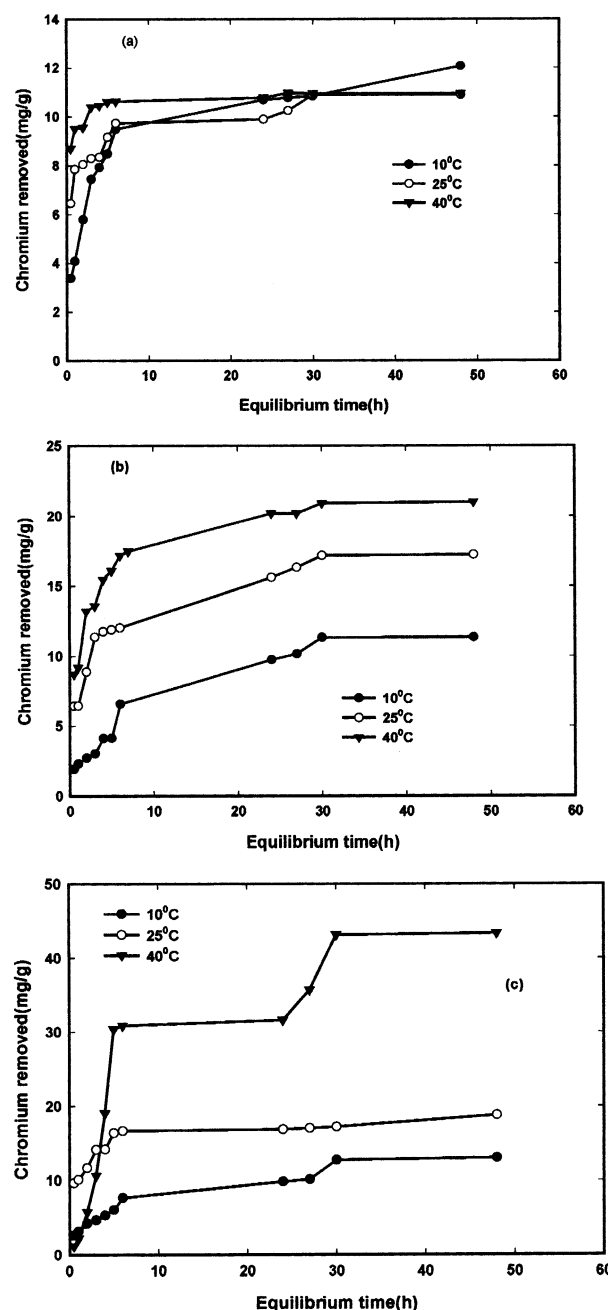
sample	10 °C			25 °C			40 °C		
	K_F (mg/g)	n	R^2	K_F (mg/g)	n	R^2	K_F (mg/g)	n	R^2
FAC	0.6941	0.6287	0.5856	2.399	0.4741	0.4768	1.317	0.5988	0.6722
SAC	0.6147	0.1718	0.2138	0.5722	0.5319	0.9479	0.3097	0.7302	0.9398
ATFAC	0.2739	0.2996	0.3825	0.5031	0.5711	0.8728	0.3648	0.6848	0.9807
ATSAC	0.7250	0.1649	0.2048	0.3456	0.6463	0.9649	0.3351	0.6841	0.9547
ACF	0.1076	1.1270	0.9546	0.1950	1.2359	0.9522	0.1327	1.4823	0.9856

Table 5. Langmuir Isotherm Constants for Cr(VI) Adsorption on Activated Carbons Derived from Agricultural Waste Materials and Activated Carbon Fabric Cloth at Different Temperatures

sample	10 °C			25 °C			40 °C		
	Q^0 (mg/g)	b (L/mg)	R^2	Q^0 (mg/g)	b (L/mg)	R^2	Q^0 (mg/g)	b (L/mg)	R^2
FAC	15.99	0.022	0.6122	21.75	0.0536	0.5485	24.11	0.0280	0.7149
SAC	1.38	0.3697	0.4492	9.535	0.0200	0.9088	32.61	0.0039	0.9239
ATFAC	1.08	0.1492	0.5015	9.866	0.0202	0.8843	15.56	0.0110	0.9747
ATSAC	1.61	0.3510	0.4508	11.51	0.0129	0.9624	16.43	0.0087	0.9434
ACF	116.92	-0.0014	0.9515	96.30	-0.0040	0.9135	42.09	0.0107	0.1778

**Figure 8.** Comparative evaluation of Langmuir and Freundlich regression coefficients for Cr(VI) removal on various adsorbents.**Figure 9.** Shapes of Langmuir isotherms obtained depending on the R_L value.

dependent on the amount of carbon. Preliminary investigations of the rate of uptake of Cr(VI) on activated carbons indicated that the processes are quite rapid and that typically 40–50% of the ultimate adsorption occurs within the first hour of contact (Figures 10 and 11). This adsorption subsequently gives way to a very slow approach to equilibrium, and in 48 h, saturation is reached. The removal of Cr(VI) was also studied at different adsorbate concentrations, viz., 25, 50, and 100 mg/L, and temperatures, viz., 10, 25, and 40 °C, at 125 rpm, and the results of these experiments are included in Figures 10 and 11. The extents of adsorption of Cr(VI) and its rates of removal on FAC and ACF are found to increase with temperature (Table 6), confirming the process to be endothermic in nature. The half-life of the adsorption process (t_{50}) decreases with increasing temperature. The amount of Cr(VI) removed in the first hour of contact increases as the concentration of the adsorbate increases. Also, the amount of Cr(VI) removed in the first hour of contact increases with increasing concentration of Cr(VI), and an increase in the initial

**Figure 10.** Effect of contact time on the rate of adsorption of Cr(VI) by activated carbon fabric cloth (ACF) at different temperatures; optimum pH; and adsorbate concentrations of (a) 25, (b) 50, and (c) 100 mg/L.

concentration of Cr(VI) enhances the sorption rate. Further, the time required for 50% of the ultimate adsorption is found to be more or less independent of the initial adsorbate concentration (Table 7).

To elucidate the adsorption mechanism, the first-order and second-order kinetic models were tested to

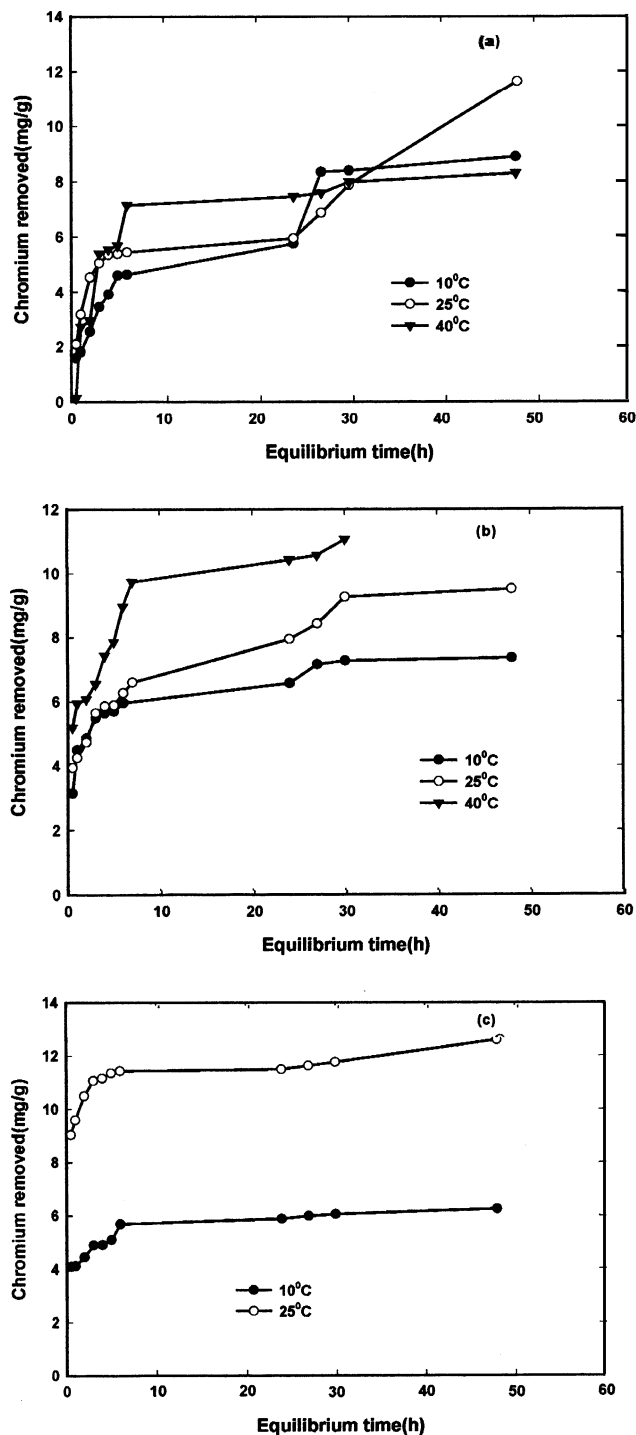


Figure 11. Effect of contact time on the rate of adsorption of Cr(VI) by activated carbon derived from coconut shell fibers without acid treatment (FAC) at different temperatures; optimum pH; and adsorbate concentrations of (a) 25, (b) 50, and (c) 100 mg/L.

fit the experimental data obtained from batch metal removal experiments. Moreover, the determination of a good fitting model could allow further water treatment process designing.

(1) Pseudo-First-Order Kinetic Model. A simple kinetic model that describes the process of adsorption is the pseudo-first-order equation as suggested by Lagergren⁴⁴ and further cited by Ho et al.⁴⁵

$$\frac{dq_t}{dt} = k_1(q_e - q_t) \quad (8)$$

where k_1 (min^{-1}) is the first-order rate constant of adsorption, q_e is the amount of chromium adsorbed at equilibrium, and q_t is the amount adsorbed at time t .

Integrating eq 8 with the initial condition $q_t = 0$ at $t = 0$, we obtain

$$\ln\left(\frac{q_e - q_t}{q_e}\right) = -k_1 t \quad (9)$$

or

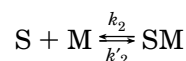
$$\log(q_e - q_t) = \log q_e - \frac{k_1}{2.303} t \quad (\text{linear form}) \quad (10)$$

or

$$q_t = q_e(1 - e^{-k_1 t}) \quad (\text{nonlinear form}) \quad (11)$$

In most of cases, the first-order equation of Lagergren did not apply throughout the complete range of contact time and was generally applicable over the initial 20–30 min of the sorption process. Plots of $\log(q_e - q_t)$ versus time (Figure 12a,b) deviated considerably from the experimental data after a short period. The slopes and intercepts as calculated from the plots were used to determine k_1 (first-order rate constant) and q_e (equilibrium capacity). The q_e values as calculated from the first-order rate equation are lower than the experimental values as obtained directly from the kinetic plots (maximum value where the equilibrium is reached). The values of k_1 and q_e together with their regression coefficients are provided in Table 6. Therefore, it can be concluded that chromium–adsorbent systems do not follow a first-order rate equation.

(2) Pseudo-Second-Order Kinetic Model. The kinetics of chromium–adsorbent systems can be represented as



where S is an active site occupied on the adsorbent (AC/ACF in the present study); M is a free metal ion (chromium in the present study) in solution; SM represents a chromium ion bound to AC/ACF; and k_2 and k'_2 are the adsorption and desorption rate constants, respectively. The kinetic equation for the adsorption process was developed by Ho and McKay and can be written as⁴⁵

$$\frac{d[S]_t}{dt} = k_2([S]_0 - [S]_t)^2 \quad (12)$$

where $[S]_0$ and $[S]_t$ are the numbers of active sites on the adsorbent at initial time $t = 0$ and time t , respectively. It is considered that sorption capacity is directly proportional to the number of active sites occupied on the activated carbons/activated carbon fabric cloth; this can be written as^{45–47}

$$\frac{dq_t}{dt} = k_2(q_e - q_t)^2 \quad (13)$$

where k_2 ($\text{g mg}^{-1} \text{h}^{-1}$) is the rate constant of pseudo-second-order adsorption, q_e is the amount of chromium adsorbed at equilibrium, and q_t is the amount adsorbed at time t .

Table 6. Pseudo-First-Order Kinetic Parameters for the Adsorption of Cr(VI) on Different Adsorbents

initial conc (mg/L)	temp (°C)	FAC				ACF			
		k_1 (min ⁻¹)	q_e (mg/g)		R^2	k_1 (min ⁻¹)	q_e (mg/g)		R^2
			equation ^a	plot ^b			equation ^a	plot ^b	
25	10	0.0777	7.2644	8.9	0.8388	0.0590	6.093	12.07	0.8687
	25	0.1950	7.6436	11.62	0.7488	0.0543	2.955	10.89	0.7764
	40	0.0810	4.6184	8.30	0.8300	0.0881	1.048	10.95	0.5893
50	10	0.0981	3.0542	7.36	0.8770	0.0780	10.61	11.36	0.7418
	25	0.0458	4.6676	9.51	0.8326	0.0466	1.113	17.25	0.6486
	40	0.0734	5.1276	11.06	0.9341	1.0500	39.15	21.01	0.6394
100	10	0.0719	1.7729	6.25	0.9024	0.1492	12.95	13.03	0.6921
	25	0.0312	2.0801	12.59	0.5807	0.1209	10.76	18.78	0.8198
	40	—	—	47.73	—	0.0783	9.210	43.38	0.8340

^a As calculated by first-order equation. ^b As calculated by kinetic plots.

Table 7. Effect of Temperature and Concentration of Adsorbate on the Rate of Uptake of Cr(VI)^a

adsorbate conc (mg/L)	temp (°C)	amount adsorbed in first hour (mg/g)	t_{50} (h)
FAC			
25	10	1.8	6.5
	25	3.1	5.0
	40	2.7	2.5
50	10	4.1	0.5
	25	9.5	2.5
	40	—	2.0
100	10	4.2	0.5
	25	4.4	0.5
	40	5.9	—
ACF			
25	10	4.0	2.0
	25	7.8	0.5
	40	9.5	0.3
50	10	2.3	5.5
	25	6.4	2.0
	40	9.1	1.5
100	10	3.1	5.0
	25	4.7	4.0
	40	10.1	2.5

^a Particle size = 200–250 mesh.

Separating the variables of eq 13 gives

$$\frac{dq_t}{(q_e - q_t)^2} = k_2 dt \quad (14)$$

Integrating eq 14, considering that $q_0 = 0$ when $t = 0$ and that $q_t = q_t$ when $t = t$, results in the expression

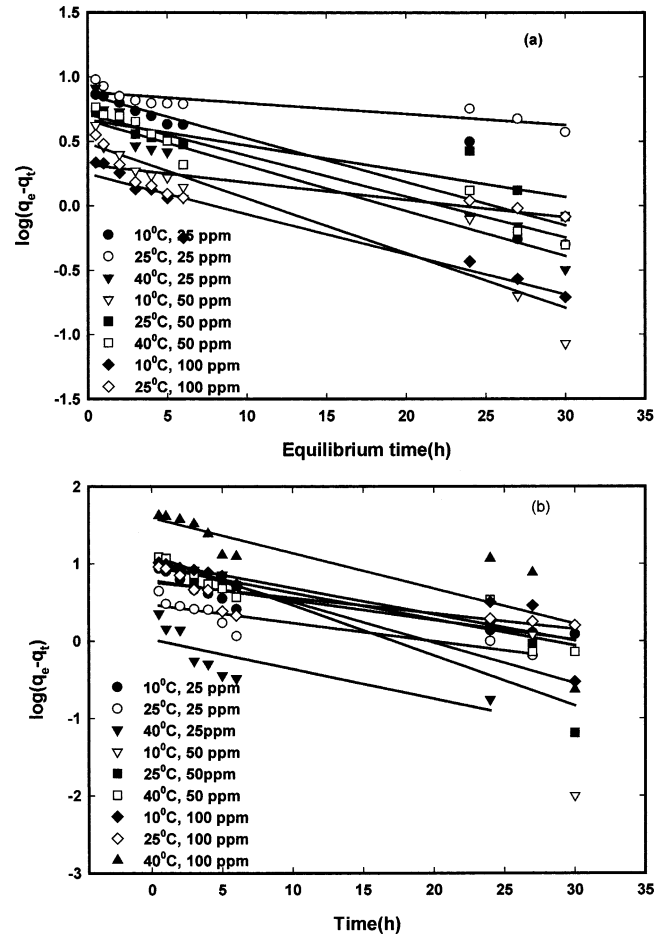
$$\frac{1}{(q_e - q_t)^2} = \frac{1}{q_e} + k_2 t \quad (15)$$

Rearranging eq 15 then gives

Table 8. Pseudo-Second-Order Kinetic Parameters for the Adsorption of Cr(VI) on Different Adsorbents

initial conc (mg/L)	temp (°C)	FAC				ACF			
		$k_2 \times 10^{-2}$ (g mg ⁻¹ h ⁻¹)	q_e (mg/g)		R^2	$k_2 \times 10^{-2}$ (g mg ⁻¹ h ⁻¹)	q_e (mg/g)		R^2
			equation ^a	plot ^b			equation ^a	plot ^b	
25	10	1.54	9.38	8.9	0.9541	8.39	12.12	12.07	0.9963
	25	2.11	9.95	11.62	0.8771	14.70	10.91	10.89	0.9979
	40	2.56	8.58	8.30	0.9969	5.97	10.99	10.95	0.9995
50	10	3.40	7.44	7.36	0.9978	3.14	13.09	11.36	0.9778
	25	3.63	9.67	9.51	0.9921	27.95	17.82	17.25	0.9978
	40	9.35	11.32	11.06	0.9970	69.25	21.59	21.01	0.9995
100	10	2.91	6.29	6.25	0.9992	5.01	13.66	13.03	0.9738
	25	33.84	12.31	12.59	0.9976	58.51	18.48	18.78	0.9965
	40	—	—	47.73	—	132.27	57.88	43.38	0.8375

^a As calculated by second-order equation. ^b As calculated by kinetic plots.

**Figure 12.** Lagergren plots for the adsorption of Cr(VI) on (a) FAC and (b) ACF at pH 2.0, at different temperatures and concentrations of adsorbate.

$$q_t = \frac{t}{\left(\frac{1}{k_2 q_e^2}\right) + \left(\frac{t}{q_e}\right)} \quad (16)$$

or

$$\frac{t}{q_t} = \frac{1}{k_2 q_e^2} + \frac{t}{q_e} \quad (17)$$

The product $k_2 q_e^2$ actually represents the initial sorption rate, i.e.

$$\text{rate} = k_2 q_e^2 \quad (18)$$

Using eq 17, t/q_t was plotted against t at different adsorbate concentrations and at different temperatures. The second-order sorption rate constant (k_2) and equilibrium absorption (q_e) values were determined from the slopes and intercepts of the plots (Figure 13 a,b). The correlation coefficients (R^2) for the linear plots are superior (in most cases ≥ 0.9950). The values of q_e and k_2 are presented in Table 8. The theoretical q_e values as calculated using the second-order rate equation agree perfectly with the experimental q_e values as determined by the kinetic plots at the equilibrium point. This suggests that the sorption system is not a first-order reaction and that a pseudo-second-order model should be considered. The pseudo-second-order model is based on the assumption that the rate-limiting step is a chemical sorption involving valance forces through the sharing or exchange of electrons between the adsorbent and adsorbate. It provides the best correlation of the data.

To interpret the experimental data, it is necessary to identify the step that governs the overall removal rate in the adsorption process. The mathematical treatments of Boyd et al.⁴⁸ and Reichenberg⁴⁹ to distinguish between particle and film diffusion and a mass-action-controlled mechanism of exchange have laid the foundations of sorption/ion exchange kinetics.

The three consecutive steps in the adsorption of an organic/inorganic species by a porous adsorbent are (1) transport of the adsorbate to the external surface of the adsorbent (film diffusion); (2) transport of the adsorbate within the pores of the adsorbent, except for a small amount of adsorption that occurs on the external surface (particle diffusion); and (3) adsorption of the adsorbate on the exterior surface of the adsorbent.

It is generally accepted that step 3 is quite rapid and does not represent the rate-determining step in the uptake of organic/inorganic compounds.³⁵ For the remaining two steps in the overall transport, three distinct cases occur: (1) case I, external transport > internal transport; (2) case II, external transport < internal transport; and (3) case III, external transport \approx internal transport

In cases I and II, the rate is governed by film and particle diffusion, respectively. In case III, the transport of ions to the boundary might not be possible at a significant rate, thereby leading to the formation of a liquid film with a concentration gradient surrounding the sorbent particles. Usually, external transport is the rate-limiting step in systems that have (a) poor mixing, (b) low concentrations of adsorbate, (c) small particle sizes, and (d) high affinity of the adsorbate for the adsorbent. In contrast, the intraparticle step limits the overall transfer for systems that have (a) high concentrations of adsorbate, (b) good mixing, (c) large adsorbent particle sizes, and (d) low affinity of the adsorbate for the adsorbent.

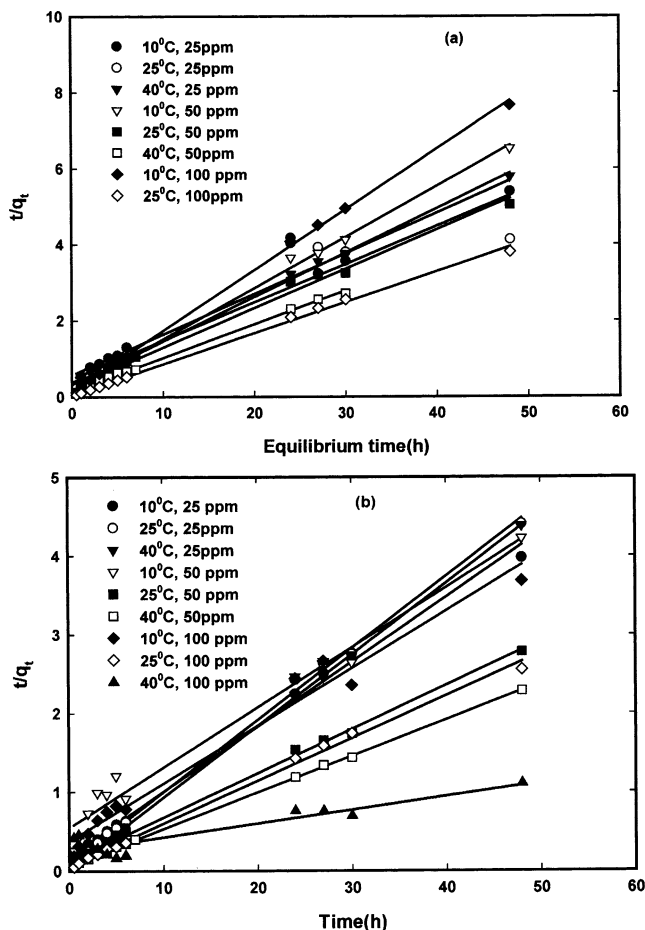


Figure 13. Pseudo-second-order kinetic plots for the adsorption of Cr(VI) on (a) FAC and (b) ACF at different initial chromium-(VI) concentrations and temperatures.

Kinetic data were analyzed by applying the mathematical model given by Reichenberg⁴⁹ and Helfferich.⁵⁰ The following equations (eqs 19–24) were used

$$F = 1 - \frac{6}{\pi^2} \sum_{n=1}^{\infty} \frac{1}{n^2} \left(\frac{-D_i t \pi^2 n^2}{r_o^2} \right) \quad (19)$$

or

$$F = 1 - \frac{6}{\pi^2} \sum_{n=1}^{\infty} \frac{1}{n^2} \exp(-n^2 B t) \quad (20)$$

where F is the fractional attainment of equilibrium at time t and is obtained from the expression

$$F = \frac{Q_t}{Q^0} \quad (21)$$

where Q_t is the amount of adsorbate taken up at time t , Q^0 is the maximum equilibrium uptake, and

$$B = \frac{\pi^2 D_i}{r_o^2} = \text{time constant} \quad (22)$$

with D_i as the effective diffusion coefficient of ion in the adsorbent phase; r_o as the radius of the adsorbent particle, assumed to be spherical; and n as an integer that defines the infinite series solution. Bt values were ob-

Table 9. Thermodynamic Parameters of Activation

adsorbate conc (mg/L)	effective diffusion coefficient, D_i (m ² s ⁻¹)			preexponential factor (D_0) (m ² s ⁻¹)	activation energy (E_a) (kJ mol ⁻¹)	activation entropy (ΔS^\ddagger) (J K ⁻¹ mol ⁻¹)
	10 °C	25 °C	40 °C			
	FAC					
25	155.79×10^{-16}	104.23×10^{-16}	198.11×10^{-16}	1.35×10^{-13}	2.37	-3.442
50	399.91×10^{-16}	154.49×10^{-16}	—	—	—	—
100	378.29×10^{-16}	525.12×10^{-16}	225.37×10^{-16}	2.56×10^{-11}	6.658	-4.923
	ACF					
25	442.23×10^{-16}	501.55×10^{-10}	891.95×10^{-16}	5.68×10^{-11}	7.39	-5.148
50	180.92×10^{-16}	183.79×10^{-10}	465.33×10^{-16}	2.51×10^{-11}	9.89	-5.567
100	94.16×10^{-16}	652.72×10^{-10}	390.39×10^{-16}	5.70×10^{-11}	15.58	-7.103

tained for each observed value of F at different temperatures and concentrations from Reichenberg's table.⁴⁹ A linearity plot of Bt versus time plots was employed to distinguish between adsorption controlled by film diffusion and particle diffusion. If a plot of Bt vs time (having slope B) is a straight line passing through the origin, then the adsorption is governed by a particle diffusion mechanism; otherwise, it is governed by film diffusion. It is interesting to note that, at different temperatures and concentrations, for FAC and ACF, the Bt vs time plots are linear and pass through the origin, except for few cases, indicating that particle diffusion mechanism is the rate-controlling step. The results for FAC and ACF at different concentrations and temperatures are plotted in Figures 14 and 15. As can be seen from Figure 14 for carbon FAC, except for the data at 100 mg/L, all plots are linear and pass through the origin, indicating that particle diffusion is the rate-determining step. In the case of ACF (Figure 15), it is interesting to note that, at low concentration, i.e., 25 mg/L the rate is governed by film diffusion in the initial hours of contact time followed by the particle diffusion. McKay plots at different adsorbate concentrations and temperatures (plots are omitted for brevity) further substantiated these findings.³⁵

The effective diffusion coefficients were estimated from the slopes of the Bt plots using eq 19. The effective diffusion coefficients as estimated from Figure 16 at different temperatures are reported in Table 9. An increase in the mobility of the ions and a decrease in the retarding forces acting on the diffusing ion result in an increase of D_i with temperature. The energy of activation, E_a ; the entropy of activation, ΔS^\ddagger , and the preexponential factor, D_0 , analogous to the Arrhenius frequency factor were also evaluated using eqs 23 and 24 and are included in Table 9

$$D_i = D_0 \exp\left[-\frac{E_a}{RT}\right] \quad (23)$$

$$D_0 = 2.72d^2 \frac{kT}{h} \exp\left(\frac{\Delta S^\ddagger}{R}\right) \quad (24)$$

where k is the Boltzmann constant; h is Planck's constant; R is the gas constant; and d is the distance between two active sites of the adsorbent, which is conventionally taken as 5 Å in inorganic ion exchangers, minerals, and other adsorbents similar to carbon. The negative ΔS^\ddagger values obtained for the adsorption of Cr(VI) on various adsorbents reflect the fact that no significant change occurs in the internal structure of the adsorbent material during adsorption. Negative ΔS^\ddagger values are not uncommon in metal adsorption.

4. Conclusions

The agricultural waste materials coconut shell and coconut shell fibers were converted into low-cost acti-

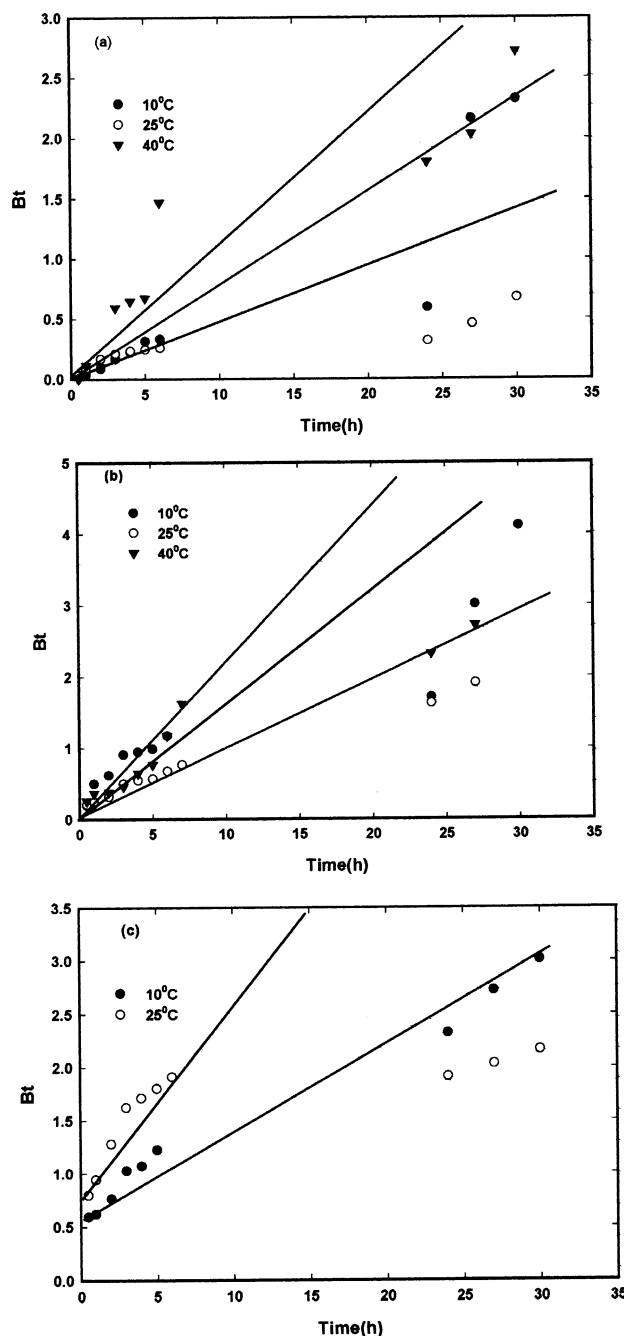


Figure 14. Bt vs time plots for Cr(VI) adsorption on FAC at initial concentrations of (a) 25, (b) 50, and (c) 100 mg/L.

vated carbons, viz., FAC, SAC, ATFAC, and ATSAC, successfully. These carbons were characterized and utilized for the removal of Cr(VI) from aqueous solution over a broad range of concentrations (1–100 mg/L). The results were found to be highly promising. Both equilibrium and kinetic studies were performed in batch

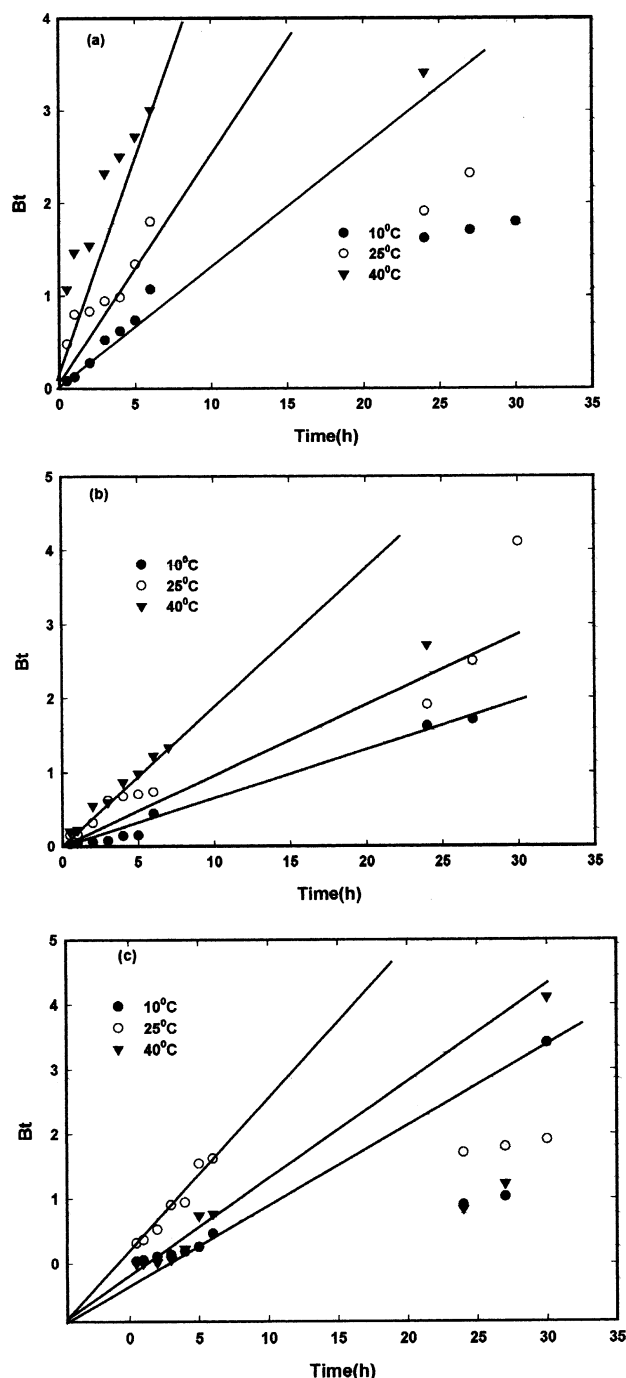


Figure 15. Bt vs time plots for Cr(VI) adsorption on ACF at initial concentrations of (a) 25, (b) 50, and (c) 100 mg/L.

mode because of its simplicity to determine various parameters necessary to establish the operation of fixed-bed reactors. The sorption data are better fitted by the Langmuir adsorption isotherm model as compared to the Freundlich model. Further, the nonlinear isotherm models better fit the data as compared to the linear ones. The monolayer capacity (Q^0) was calculated using the Langmuir adsorption isotherm for the activated carbons FAC, SAC, ATFAC, ATSAC, and ACF and was found to increase with increasing temperature, confirming the endothermic nature of the process. Also, the sorption capacity was found to be comparable (Table 10) to those of commercially available activated carbons and low-cost adsorbents used for the remediation of Cr(VI) from water/wastewater. The removal of Cr(VI) follows the order $ACF > FAC > ATSAC > ATFAC > SAC$.

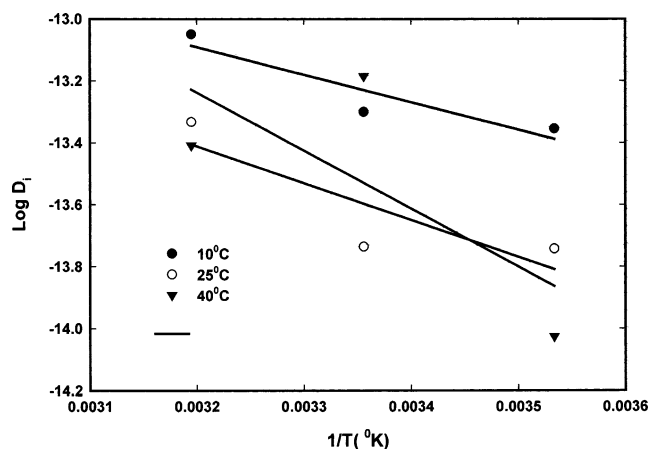


Figure 16. $\log(D_i)$ vs $1/T$ plots for Cr(VI) adsorption on ACF.

Table 10. Adsorption Capacities of the Developed Adsorbents Compared to Other Adsorbents

activated carbon/adsorbent	adsorption capacity (mg/g)	ref
fly ash	1.2	51
iron-coated spent catalyst	0.720	52
polyacrylamide-grafted saw dust	12.4	53
blast furnace slag	1.5	26
commercial activated carbon	~12	14
saw dust	40.0	54
sugar beet pulp	17.2	54
maize cob	14.0	54
sugar cane bagasse	13.4	54
walnut shell	1.33	55
waste tea	1.55	55
activated carbon M	3.9	22
activated carbon M-B	3.3	22
chabazite	3.60	56
clinoptilolite	2.40	56
as-received CSC	2.18	31
as-received CAC	4.72	31
nitric oxide CSC	10.88	31
nitric oxide CAC	15.47	31
anatase (TiO ₂)	14.56	57
coconut tree sawdust	3.46	58
red Mud	1.60	59
saw dust	3.30	60
FAC	21.75	this study
SAC	9.53	this study
ATFAC	9.86	this study
ATSAC	11.51	this study
ACF	22.29	this study

Overall, the activated carbon fabric cloth performed better than the other tested adsorbents.

The rate of the adsorption is governed by a pseudo-second-order rate equation. Further, the adsorption of Cr(VI) is controlled by a particle diffusion mechanism in a majority of cases. Column studies to investigate the hydrodynamic and chemical characteristics of adsorption in a flow-through system and regeneration of the adsorbents without dismantling the same are in progress based on these findings. It can be concluded that the coconut shells/fibers commodity group will benefit from this research because it will add value to surplus byproducts. Carbon users would also be benefited because this material offers a viable alternative to coal-based activated carbons. Thus, the studies presented here reveal that the derived low-cost activated carbons could be fruitfully employed as adsorbents for the removal of chromium from aqueous solution without any sludge production. Studies with actual tannery wastewater are in progress.

Acknowledgment

The authors are thankful to the Director, Industrial Toxicology Research Centre, Lucknow, India, for providing all necessary facilities for this work and consistent encouragement and guidance throughout this work. The authors are also very thankful to Professor Vicente Gomez Serrano, Universidad Extremadura, Extremadura, Spain, for helping in the surface characterization of the prepared adsorbents.

Literature Cited

- (1) Tiravanti, G.; Petruzzelli, D.; Passino, R. Pretreatment of tannery wastewaters by an ion exchange process for Cr(III) removal and recovery. *Water Sci. Technol.* **1997**, *36*, 197.
- (2) Rengaraj, S.; Joo, C. K.; Kim, Y.; Yi, J. Kinetics of removal of chromium from water and electronic process wastewater by ion-exchange resins: 1200H, 1500H and IRN97H. *J. Haz. Mater.* **2003**, *102* (2–3), 257.
- (3) Seaman, J. C.; Bertsch, P. M.; Schwallie, L. In situ Cr(VI) reduction within coarse-textured, oxide-coated soil and aquifer systems using Fe(II) solutions. *Environ. Sci. Technol.* **1999**, *33*, 938.
- (4) Zhou, X.; Korenaga, T.; Takahashi, T.; Moriwake, T.; Shinoda, S. A process monitoring/controlling system for the treatment of wastewater containing chromium(VI). *Water Res.* **1993**, *27*, 1049.
- (5) Kozłowski, C. A.; Walkowiak, W. Removal of chromium(VI) from aqueous solutions by polymer inclusion membranes. *Water Res.* **2002**, *36* (19), 4870.
- (6) Chakravarti, A. K.; Chowdhury, S. B.; Chakrabarty, S.; Chakrabarty, T.; Mukherjee, D. C. Liquid membrane multiple emulsion process of chromium(VI) separation from wastewaters. *Colloids Surf. A: Physicochem. Eng. Aspects* **1995**, *103*, 59.
- (7) Dahbi, S.; Azzi, M.; Guardia, M. Removal of hexavalent chromium from wastewaters by bone charcoal. *Fresenius J. Anal. Chem.* **1999**, *363*, 404.
- (8) Hung, C. P.; Wu, M. H. The removal of chromium(VI) from dilute solution by activated carbon. *Water Res.* **1977**, *11*, 673.
- (9) Kongsricharoen, N.; Polprasert, C. Chromium removal by a bipolar electrochemical precipitation process. *Water Sci. Technol.* **1996**, *34*, 109.
- (10) Pagilla, K.; Canter, L. W. Laboratory studies on remediation of chromium-contaminated soils. *J. Environ. Eng.* **1999**, *125*(3), 243.
- (11) Lin, C. F.; Rou, W.; Lo, K. S. Treatment strategy for Cr(VI)-bearing wastes. *Water Sci. Technol.* **1992**, *26*, 2301.
- (12) Sawada, A.; Mori, K.; Tanaka, S.; Fukushima, M.; Tatsumi, K. Removal of Cr(VI) from contaminated soil by electrokinetic remediation. *Waste Manage.* **2004**, *24* (5), 483–490.
- (13) Lalvani, S. B.; Wiltowski, T.; Hubner, A.; Wetson, A.; Mandich, N. Removal of hexavalent chromium and metal cations by selective and novel carbon adsorbent. *Carbon* **1998**, *36* (7–8), 1219.
- (14) Leyva-Ramos, R.; Martinez, J.; Guerrero-Coronado, R. Adsorption of Cr(VI) from aqueous solutions onto activated carbon. *Water Sci. Technol.* **1994**, *30* (9), 191.
- (15) Ibanez, J. P.; Umetsu, Y. Uptake of trivalent chromium from aqueous solution using protonated dry alginate beds. *Hydrometallurgy* **2004**, *72*, 327–334.
- (16) Chun, Li; Hongzhang, C.; Zuohu, L. Adsorptive removal of Cr(VI) by Fe-modified steam exploded wheat straw. *Process Biochem.* **2004**, *39*, 541.
- (17) Bello, G.; Cid, R.; Garcia, R.; Renan, A. Retention of Cr(VI) and Hg(II) in Eucalyptus globulus and peach stone-activated carbons. *J. Chem. Technol. Biotechnol.* **1999**, *74*, 904.
- (18) Selomulya, C.; Meeyoo, V.; Amal, R. Mechanisms of Cr(VI) removal from water by various types of activated carbons. *J. Chem. Technol. Biotechnol.* **1999**, *74*, 111.
- (19) Guo, Y.; Qi, J.; Yang, S.; Yu, K.; Wang, Z.; Xu, H. Adsorption of Cr(VI) on micro- and mesoporous rice husk based active carbon. *Mater. Chem. Phys.* **2002**, *78*, 132.
- (20) Srivastava, S. K.; Gupta, V. K.; Mohan, D. Kinetic parameters for the removal of lead and chromium from wastewater using activated carbon developed from fertilizer waste material. *Environ. Model. Assess.* **1997**, *1* (4), 281.
- (21) Boddu, V. M.; Abburi, K.; Talbott, J. L.; Smith, E. D. Removal of hexavalent chromium from wastewater using a new composite chitosan biosorbent. *Environ. Sci. Technol.* **2003**, *37*, 4449.
- (22) Rivera-Utrilla, J.; Toledo, I. B.; Ferro-Garcia, M. A.; Moreno-Satilla, C.; Biosorption of Pb(II), Cd(II), and Cr(VI) on activated carbon from aqueous solutions. *Carbon* **2003**, *41*, 323.
- (23) Gupta, V. K.; Shrivastava, A. K.; Jain, N. Biosorption of Chromium(VI) from Aqueous solutions by green algae *spirogyra* species. *Water Res.* **2001**, *35* (17), 4079.
- (24) Aksu, Z.; Acikel, U.; Kabasakal, E.; Tezer, S. Equilibrium modelling of individual and simultaneous biosorption of chromium(VI) and nickel(II) onto dried activated sludge. *Water Res.* **2002**, *36*, 3063.
- (25) Gupta, V. K.; Park, K. T.; Sharma, S.; Mohan, D. Removal of chromium(VI) from electroplating industry wastewater using bagasse flyash—A sugar industry waste material. *Environmental-ist* **1999**, *19*, 129.
- (26) Srivastava, S. K.; Gupta, V. K.; Mohan, D. Removal of lead and chromium by activated slag—A blast furnace waste. *J. Environ. Eng.* **1997**, *123* (5), 461.
- (27) Lakatos, J.; Brown, S. D.; Snape, C. E. Coals as sorbents for the removal and reduction of hexavalent chromium from aqueous waste streams. *Fuel* **2002**, *81* (5), 691.
- (28) Namasivayam, C.; Yamuna, R. T. Adsorption of chromium(VI) by a low-cost adsorbent: Biogas residual slurry. *Chemosphere* **1995**, *30*, 561.
- (29) Kiyak, B.; Özer, A.; Altundogan, H. S.; Erdem, M.; Tümen, F. Cr(VI) reduction in aqueous solutions by using copper smelter slag. *Waste Manage.* **1999**, *19* (5), 333.
- (30) Gupta, V. K.; Gupta, M.; Sharma, S. Process development for the removal of lead and chromium from aqueous solutions using red mud—An aluminium industry waste. *Water Res.* **2001**, *35* (5), 1125.
- (31) Babel, S.; Kurniawan, T. A. Cr(VI) removal from synthetic wastewater using coconut shell charcoal and commercial activated carbon modified with oxidizing agents and/or chitosan. *Chemosphere* **2004**, *54*, 951.
- (32) Mohan, D.; Singh, K. P.; Sinha, S.; Gosh, D. Removal of Pyridine from aqueous solution using low cost activated carbon derived from agricultural waste materials. *Carbon* **2004**, *42*, 2409–2421.
- (33) Mohan D.; Singh, K. P.; Singh, G.; Kumar, K. Removal of dyes from wastewater using flyash, a low-cost adsorbent. *Ind. Eng. Chem. Res.* **2002**, *41*, 3688.
- (34) Mohan, D.; Singh, K. P. Single and multicomponent adsorption of zinc and cadmium from wastewater using activated carbon derived from bagasse—an agricultural waste material. *Water Res.* **2002**, *36* (9), 2302.
- (35) Mohan D.; Srivastava, S. K.; Gupta V. K.; Chander, S. Kinetics of mercury adsorption from wastewater using activated carbon derived from fertilizer waste material. *Colloids Surf. A* **2001**, *177*, 169.
- (36) Sivasamy A.; Singh K. P.; Mohan, D.; Maruthamuthu, M. Studies on defluoridation of water by coal-based sorbents. *J. Chem. Technol. Biotechnol.* **2001**, *76* (7), 717.
- (37) Singh, K. P.; Mohan, D.; Tandon, G. S.; Gosh, D. Color removal from wastewater using low-cost activated carbon derived from agricultural waste material. *Ind. Eng. Chem. Res.* **2003**, *42*, 1965.
- (38) Vogel, A. I. *A Textbook of Quantitative Chemical Analysis*, 5th ed.; ELBS Publication: London, 1989.
- (39) Singh, K. P.; Mohan, D.; Tandon, G. S.; Gupta, G. S. D. Vapor phase adsorption of hexane and benzene on activated carbon fabric cloth: Equilibria and rate studies. *Ind. Eng. Chem. Res.* **2002**, *41*, 2480.
- (40) Sengupta, A. K.; Clifford, D. Some unique characteristics of chromate ion exchange. *React. Polym.* **1986**, *4*, 113.
- (41) Jayson, G. G.; Sangster, J. A.; Thompson, G.; Wilkinson, M. C. Adsorption of chromium from aqueous solution onto activated carbon cloth. *Carbon* **1993**, *31* (3), 487.
- (42) Rodovic, L. R.; Moreno-Castilla, C.; Rivera-Utrilla, J. Carbon materials as adsorbents in aqueous solutions. In *Chemistry and Physics of Carbon*; Radovic, L. R., Ed.; Marcel Dekker: New York, 2000; p 27.

- (43) Weber, T. W.; Chackravorti, R. K. Pore and Solid Diffusion Models for Fixed Bed Adsorbers. *J. Am. Inst. Chem. Eng.* **1974**, 20, 228.
- (44) Lagergren, S. Zur theorie der sogenannten adsorption geloster stoffe (On the theory of so-called adsorption of soluble substances). *Kungliga Svenska Vetenskapsakademiens Handlingar* **1898**, 24 (4), 1.
- (45) Ho, Y. S.; McKay, G. Pseudo-second order model for sorption processes. *Process Biochem.* **1999**, 34, 451.
- (46) Hamadi, N. K.; Chen X. D.; Farid, M. M.; Lu, M. G. Q. Adsorption kinetics for removal of Cr(VI) from aqueous solution by adsorbents derived from used tyres and saw dust. *Chem. Eng. J.* **2001**, 84, 95.
- (47) Cheung, C. W.; Porter, J. F.; McKay, G. Sorption kinetics for the removal of copper and zinc from effluents using bone char. *Sep. Pur. Technol.* **2000**, 19, 55.
- (48) Boyd, G. E.; Adamson, A. W.; Mayers, L. S. The exchange adsorption of ions from aqueous solution by organic zeolites. II. Kinetics. *J. Am. Chem. Soc.* **1974**, 69, 2836.
- (49) Reichenberg, D. Properties of ion-exchange resin in relation to their structure. III Kinetics of exchange. *J. Am. Chem. Soc.* **1953**, 75, 589.
- (50) Helfferich, F. *Ion Exchange*; McGraw-Hill: New York, 1962.
- (51) Flytianos, K.; Vondrias, E.; Tsechpenakis, A. Removal of Cr(VI) from aqueous and wastewater sample by fly ash. *J. Environ. Sci. Health* **1998**, A32 (9–10), 2419.
- (52) Liu, J. C.; Huang, J. G. Using iron-coated spent catalyst as an alternative adsorbent to remove Cr(VI) from water. *Water Sci. Technol.* **1998**, 38 (4–5), 155.
- (53) Raji, C.; Anirudhan, T. S. Batch Cr(VI) removal by polyacrylamide grafted saw dust: Kinetics and thermodynamics. *Water Res.* **1998**, 32 (12), 3772.
- (54) Sharma, D. C.; Forster, C. F. Removal of hexavalent chromium, using sphagnum moss peat. *Water Res.* **1993**, 27, 1201.
- (55) Orhan, Y.; Buyukgungor, H. The removal of heavy metals by using agricultural wastes. *Water Sci. Technol.* **1993**, 28 (2), 247.
- (56) Ouki, S. K.; Kavannagh, M.; Performance of natural zeolites for the treatment of mixed metal-contaminated effluents. *Waste Manage. Res.* **1997**, 15, 383.
- (57) Weng, C. H.; Wang, J. H.; Hunag, C. P. Adsorption of Cr(VI) onto TiO₂ from dilute aqueous solutions. *Water Sci. Technol.* **1997**, 35, 55.
- (58) Selvi, K.; Pattabi, S.; Kadirvelu, K. Removal of Cr(VI) from aqueous solution by adsorption onto activated carbon. *Bioresour. Technol.* **2001**, 80, 87.
- (59) Pradhan, J.; Das, S. N.; Thakur, R. S. Adsorption of hexavalent chromium from aqueous solution by using activated red mud. *J. Colloid Interface Sci.* **1999**, 217, 137.
- (60) Srivastava, H. C. P.; Mathur R. P.; Mehrotra, I. Removal of chromium from industrial effluents by adsorption on saw dust. *Environ. Technol. Lett.* **1986**, 755.

Received for review March 17, 2004

Revised manuscript received July 20, 2004

Accepted August 7, 2004

IE0400898